Available online at www.sciencedirect.com
SCIENCE DIRECT®
International Journal of Thermal Sciences 41 (2002) 1045–1053
International Journal of Thermal Sciences
www.elsevier.com/locate/ijts

Three-dimensional analyses of double diffusive convection in a two-layer system at high Rayleigh number

Katsuyoshi Kamakura [a,*], Hiroyuki Ozoe [b]

[a] *Toyama National College of Technology, 13 Hongo-machi, Toyama 939-8630, Japan*
[b] *Institute of Advanced Material Study, Kyushu University, 6-1 Kasuga Koen, Kasuga 816-8580, Japan*

Received 18 August 2001; accepted 19 November 2001

Abstract

Three-dimensional numerical computations of double diffusive natural convection were carried out at the Prandtl number $Pr = 6$, the Lewis number $Le = 100$, the aspect ratio $A = 2$, the Rayleigh number $Ra = 10^7$ and various buoyancy ratios N for a two-layer system which consists of a pure water (upper layer) and an aqueous solution (lower layer) with lateral heating and cooling. Salt-fingers with the termination of bulbous shapes were formed owing to the penetration of convective flow in a layer into the other layer at $N = 0.3$ and plumes were formed by the collision of solutal fragments against the interface at $N = 0.6$ or 1.

Keywords: Natural convection; Double diffusion; Salt-finger; Plume; Lateral heating; Two-layer system

1. Introduction

Double diffusive natural convection occurs owing to both temperature and concentration differences under a gravitational field and then forms various phenomena such as multi-layered convection, concentration stratification, plumes and salt-fingers. These phenomena may occur in processes such as melting or freezing of ice in a aqueous solution, electrode reactions in a solution, etc. and have a profound affect upon the mixing process of a solute. When an aqueous solution having a concentration gradient along the gravitational direction is heated from a side wall and cooled from an opposing side wall, convection roll cells are formed with multiple horizontal boundaries. The simplest model for this phenomenon is a two-layer convection system [1,2]. When a two-layer system which consists of water (upper layer) and an aqueous solution (lower layer) is heated from one side and cooled from an opposite side, convection starts in each layer, and a sharp horizontal interface is formed by two flows circulating in opposite directions near the interface. The heat transfer appears to become soon approximately steady, but the mass transfer stays unsteady.

We previously reported experimental studies [1] of the double-diffusive two-layer convection as shown in Fig. 1. The experimental conditions were as follows:

- Initial upper layer: water, 8 cm in height;
- Initial lower layer: 10 kg·m^{-3} KCl solution, 8 cm in height;
- Heating temperature: 30 °C;
- Cooling temperature: 20 °C;
- System sizes: 4 cm (width) × 16 cm (height);
- Depth of the apparatus: 10 cm.

Corresponding dimensionless values are as follows.

- Aspect ratio $A = 4$;
- Prandtl number $Pr = 6.27$;
- Rayleigh number $Ra = 1.13 \times 10^7$ (by the definition of Ra in this paper);
- Lewis number $Le = 71.8$;
- Buoyancy ratio $N = 2.74$.

* Corresponding author.
E-mail addresses: kama@toyama-nct.ac.jp (K. Kamakura), ozoe@cm.kyushu-u.ac.jp (H. Ozoe).

1290-0729/02/$ – see front matter
PII: S1290-0729(02)01391-1

Nomenclature

A	aspect ratio $= h/b$		
b	width of the system	m	
B	dimensionless width of the system		
C	dimensionless concentration $= (c - c_{\min})/(c_{\max} - c_{\min})$		
c	concentration	$\mathrm{kg{\cdot}m^{-3}}$	
$c_{\max}$	initial maximum concentration (initial concentration in a lower layer)	$\mathrm{kg{\cdot}m^{-3}}$	
$c_{\min}$	initial minimum concentration (initial concentration in an upper layer)	$\mathrm{kg{\cdot}m^{-3}}$	
D	diffusion coefficient	$\mathrm{m^2{\cdot}s^{-1}}$	
g	acceleration due to gravity	$\mathrm{m{\cdot}s^{-2}}$	
h	height of the system	m	
H	dimensionless height of the system		
Le	Lewis number $= \kappa/D$		
N	buoyancy ratio $= \beta(c_{\max} - c_{\min})/\{\alpha(T_{\mathrm{hot}} - T_{\mathrm{cold}})\}$		
Nu_{ave}	average Nusselt number		
p	pressure	Pa	
P	dimensionless pressure		
Pr	Prandtl number $= \nu/\kappa$		
Ra	Rayleigh number $= g\alpha(T_{\mathrm{hot}} - T_{\mathrm{cold}})b^3/(\kappa\nu)$		
T	temperature	K	
T_{cold}	temperature on the cold wall	K	
T_{hot}	temperature on the hot wall	K	
t	time	s	
U, V	dimensionless velocity		
X, Y	dimensionless coordinate		

Greek symbols

α	volumetric coefficient of thermal expansion	$\mathrm{K^{-1}}$
β	volumetric coefficient of expansion with concentration	$\mathrm{m^3{\cdot}kg^{-1}}$
$\Delta\tau$	dimensionless time step	
θ	dimensionless temperature $= (T - T_{\mathrm{cold}})/(T_{\mathrm{hot}} - T_{\mathrm{cold}})$	
κ	thermal diffusivity	$\mathrm{m^2{\cdot}s^{-1}}$
ν	kinematic viscosity	$\mathrm{m^2{\cdot}s^{-1}}$
ρ	density	$\mathrm{kg{\cdot}m^{-3}}$
τ	dimensionless time	
ψ	dimensionless stream-function ($U = \partial\psi/\partial Y$, $V = -\partial\psi/\partial X$)	

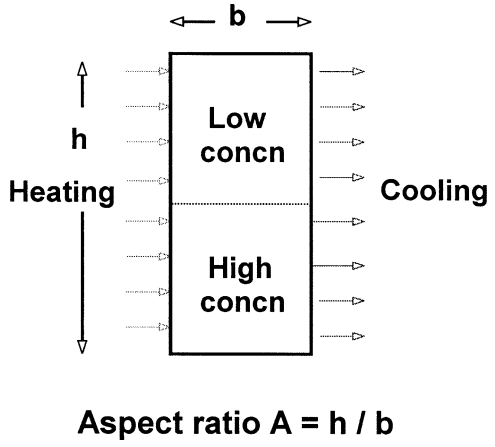

Fig. 1. Schematic illustration of two-layer system.

With such an arrangement, the concentration difference between the two layers becomes small with time, and the interface becomes unstable. Phenomena such as wavering of interface and a large slope of interface are observed as shown in Fig. 2. The fluid near the wall finally streamed into the other layer and the two-layer system changed into a one-layer system.

Bergman and Ungan [3] carried out similar experiments for a low concentration difference between two layers. In the final stages before mixing, the hydrodynamic boundary layers on the heated and cooled sidewalls penetrate the salinity interface and mixing, in the finger regime, occurs. Chen and Chen [3] observed salt-fingers for the system of a solute gradient subjected to lateral heating. Tanny and Yakubov [4] reported an experimental study that revealed when the flow adjacent to the interface is unstable, the mixing process is characterized by intense vortices.

Hyun and Bergman [5] carried out a numerical 2D simulation of the above phenomenon. The results indicated two mechanisms that lead to the destruction of the salinity interface. At low Rayleigh numbers thermal convection gradually and smoothly peels high (or low) saline water from the interface and folds it into the convective layer. At higher Rayleigh numbers, an intermittent mechanism is predicted to occur with solutal plumes, carried in full circle by thermal convection, bombarding the interface and ejecting fluid into the convecting layers. Nishimura et al. [6] studied the mechanism of cell merging, and buoyancy plumes perpendicular to shear flows due to diffusive instabilities are periodically generated from the interface.

In this paper, numerical studies are carried out for different buoyancy ratios $N = 0$, 0.3, 0.6, 1 and 3 which correspond to the small or middle concentration difference between layers. Three-dimensional system behavior was presumed. A finite difference method was employed for the numerical analyses of this two-layer convection system. Unequal meshes were employed with minute ones near a central interface area.

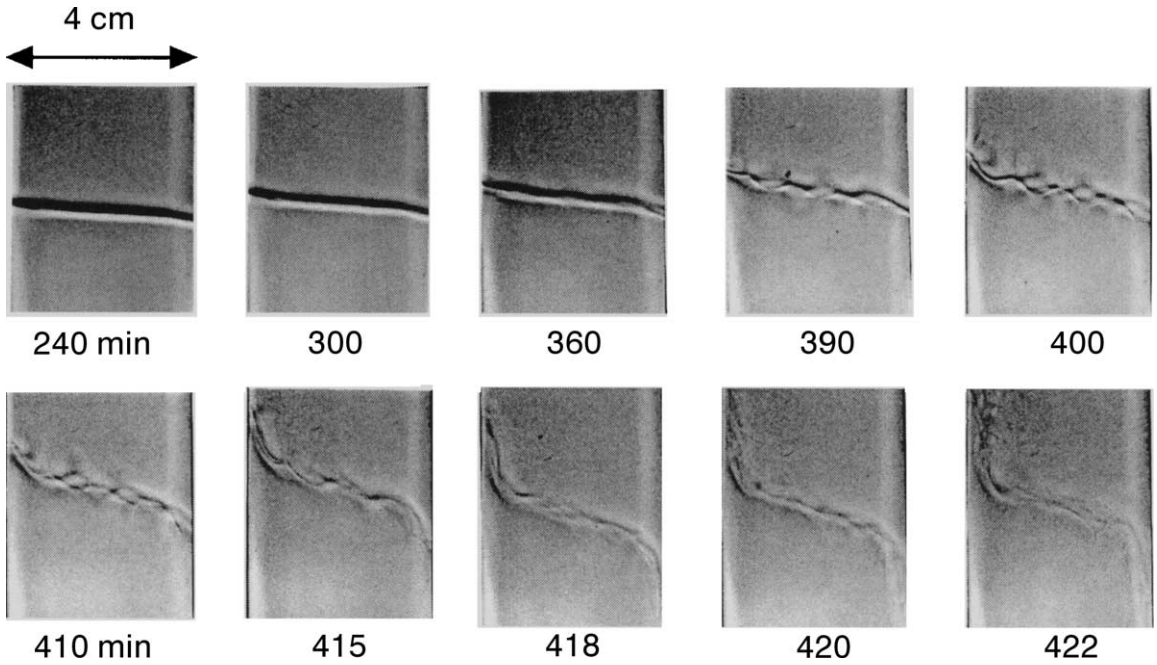

Fig. 2. Shadowgraphs of the interface between two convection layers. The time is the elapsed time from the start of heating and cooling. Upper layer: water, lower layer: 10 kg·m^{-3} KCl solution, heating: 30 °C (left hand), cooling: 20 °C (right hand), aspect ratio 4.

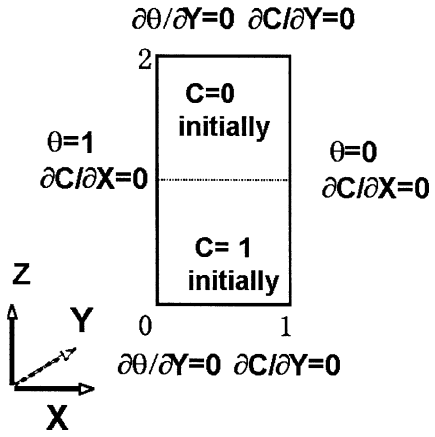

Fig. 3. Boundary conditions.

2. Numerical analysis

2.1. Mathematical model

The model equations to describe the double diffusive natural convection as shown in Fig. 1 consist of the continuity, the Navier–Stokes, the energy and the concentration equations in dimensionless forms as follows:

$$\nabla \cdot \boldsymbol{V} = 0 \tag{1}$$

$$\partial \boldsymbol{V}/\partial\tau + (\boldsymbol{V}\cdot\nabla)\boldsymbol{V} = -\nabla P + Pr\nabla^2\boldsymbol{V} + Pr\,Ra(\theta - NC)\boldsymbol{k} \tag{2}$$

$$\partial\theta/\partial\tau + (\boldsymbol{V}\cdot\nabla)\theta = \nabla^2\theta \tag{3}$$

$$\partial C/\partial\tau + (\boldsymbol{V}\cdot\nabla)C = \nabla^2 C/Le \tag{4}$$

Dimensionless parameters *Pr*, *Ra*, *Le*, *N* and *A* are defined as follows:

$$Pr = \frac{\nu}{\kappa}, \qquad Ra = \frac{g\alpha(T_{\mathrm{hot}} - T_{\mathrm{cold}})b^3}{\kappa\nu}$$
$$Le = \frac{\kappa}{D}, \qquad N = \frac{\beta(c_{\max} - c_{\min})}{\alpha(T_{\mathrm{hot}} - T_{\mathrm{cold}})}, \qquad A = \frac{h}{b} \tag{5}$$

Here, the dimensionless variables are defined as follows:

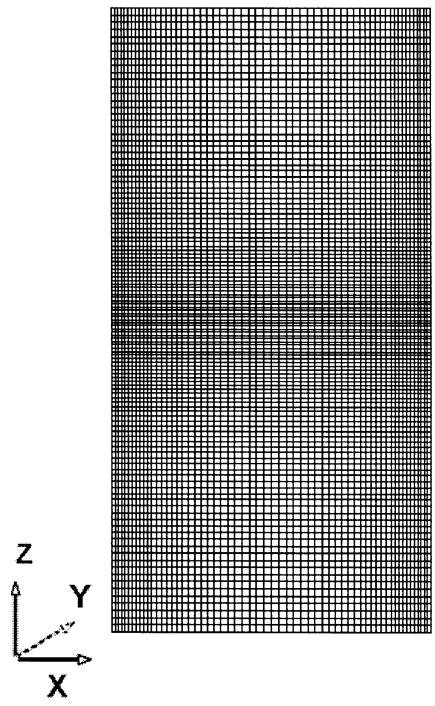

Fig. 4. Mesh of XZ-plane (61 × 121 grid points) for 3D calculation. The grid points in the Y-direction are 61 and positioned with a constant spacing.

$$X = x/b, \qquad Y = y/b, \qquad Z = z/b$$
$$U = ub/\kappa, \qquad V = vb/\kappa, \qquad W = wb/\kappa$$
$$\tau = t\kappa/b^2, \qquad P = pb^2/(\rho\kappa^2)$$

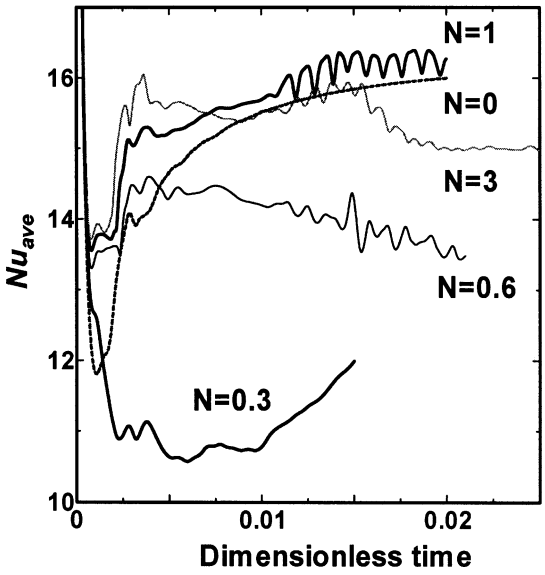

Fig. 5. Variation of Nu_{ave} on the hot wall with time at $Pr = 6$, $Le = 100$, $A = 2$ and $Ra = 10^7$.

$$\theta = \frac{(T - T_{cold})}{(T_{hot} - T_{cold})}, \qquad C = \frac{(c - c_{min})}{(c_{max} - c_{min})}$$

2.2. Boundary conditions

The boundary conditions in dimensionless form are illustrated in Fig. 3.

at $X = 0$, $U = V = W = 0$, $\theta = 1$, $\partial C/\partial X = 0$
at $X = 1$, $U = V = W = 0$, $\theta = 0$, $\partial C/\partial X = 0$
at $Y = 0$, $U = V = W = 0$, $\partial\theta/\partial Y = 0$, $\partial C/\partial Y = 0$
at $Y = 1$, $U = V = W = 0$, $\partial\theta/\partial Y = 0$, $\partial C/\partial Y = 0$
at $Z = 0$, $U = V = W = 0$, $\partial\theta/\partial Z = 0$, $\partial C/\partial Z = 0$
at $Z = 2$, $U = V = W = 0$, $\partial\theta/\partial Z = 0$, $\partial C/\partial Z = 0$

The initial temperature in the system is 0.5 and the initial concentration is 0 in the upper layer and 1 in the lower layer.

2.3. Computation

A finite difference method was employed to solve the model equations numerically. The calculation algorithm of pressure terms is the HSMAC method. The third order upwind scheme (Utopia scheme [7]) for the inertial terms of Eqs. (2)–(4) was applied to the calculation. The local Nusselt number on the hot wall was calculated from a Taylor series for the temperature field and the average Nusselt number was computed by an integration over the hot wall. Computations

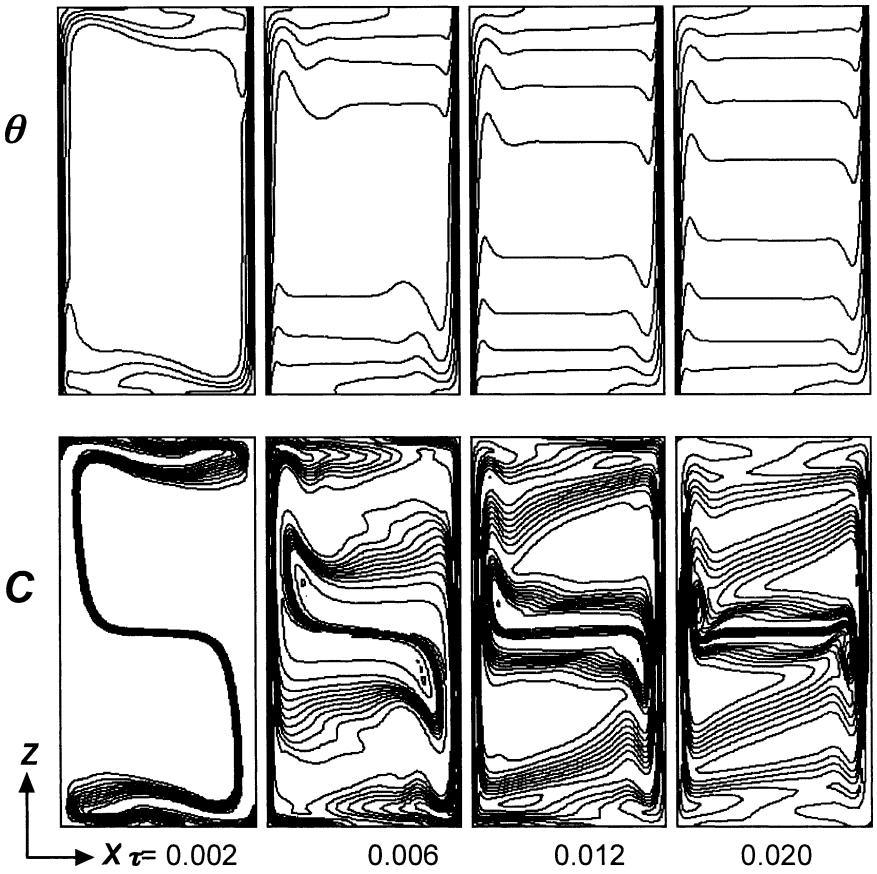

Fig. 6. Instantaneous contours at $N = 0$ and 0.3.

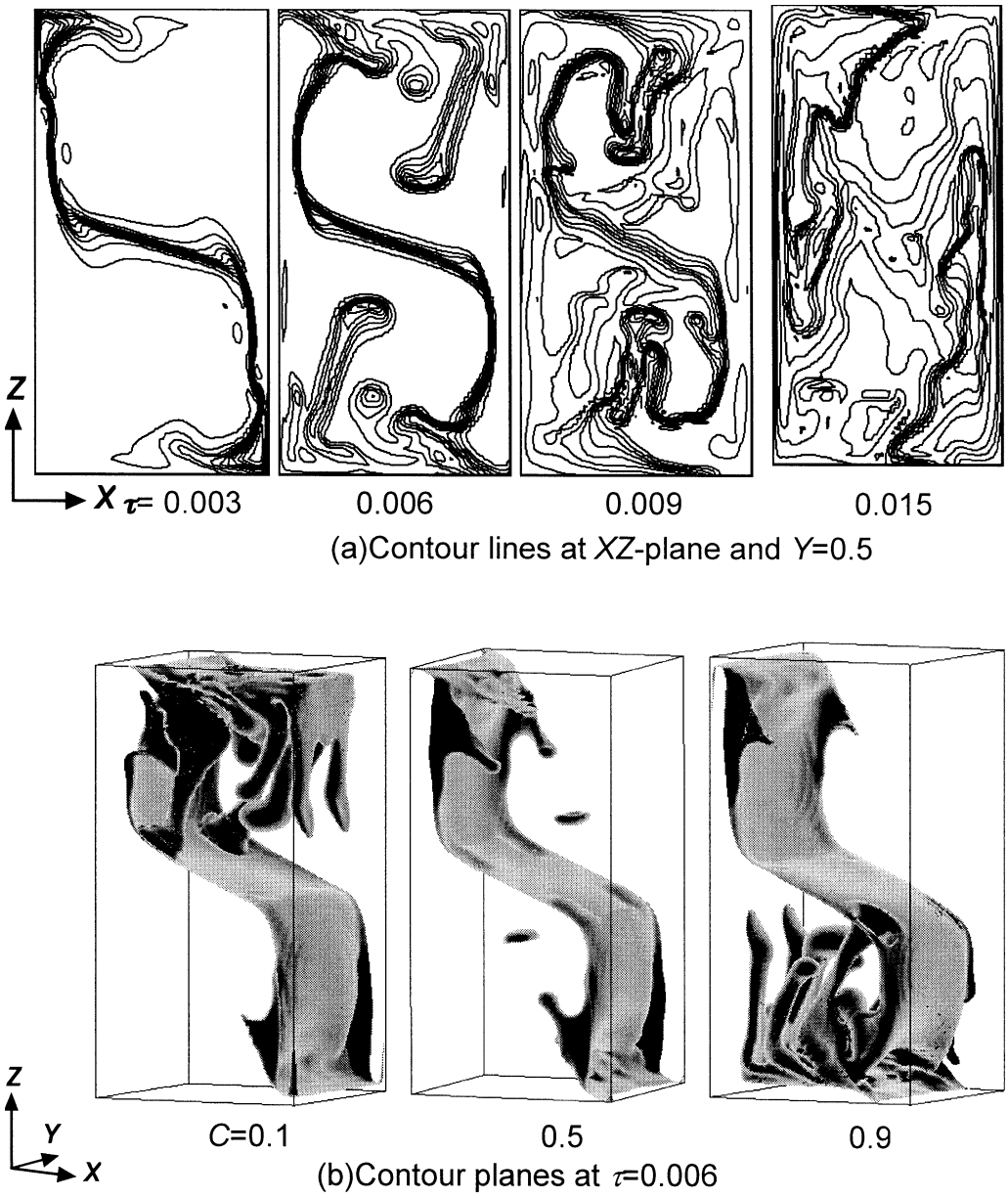

Fig. 7. Concentration distribution at $N = 0.3$.

were carried out by a personal computer. The time step width $\Delta\tau$ was 1×10^{-7}.

2.4. Computational meshes

The computational meshes were refined in the vicinity of a horizontal central height ($Z = 1$) and near the vertical walls as shown in Fig. 4. The finite difference grid points in the X-, Y- and Z-directions were $61 \times 61 \times 121$. The grid points in the X-direction are positioned according to

$$\frac{X_i}{B} = \frac{i}{i_{\max}} - \frac{\alpha_X}{2\pi}\sin\left(2\pi\frac{i}{i_{\max}}\right) \quad i = 0, 1, 2, \ldots, i_{\max} \quad (6)$$

where α_X is 0.4. All the grid points in the Y-direction are positioned with a constant spacing. The grid points in the Z-direction are defined to be symmetrical in terms of $Z = 1$. First the grid points in the Z-direction were calculated at $\alpha_Z = 0.8$ similarly to the case of X-direction. Next the lower half grid points moved to the upper layer and the original upper half grid points moved to the lower layer.

3. Results and discussion

3.1. Oscillatory phenomena

The oscillatory phenomena of double diffusive convection in a two-layer system was reported by Kamakura and

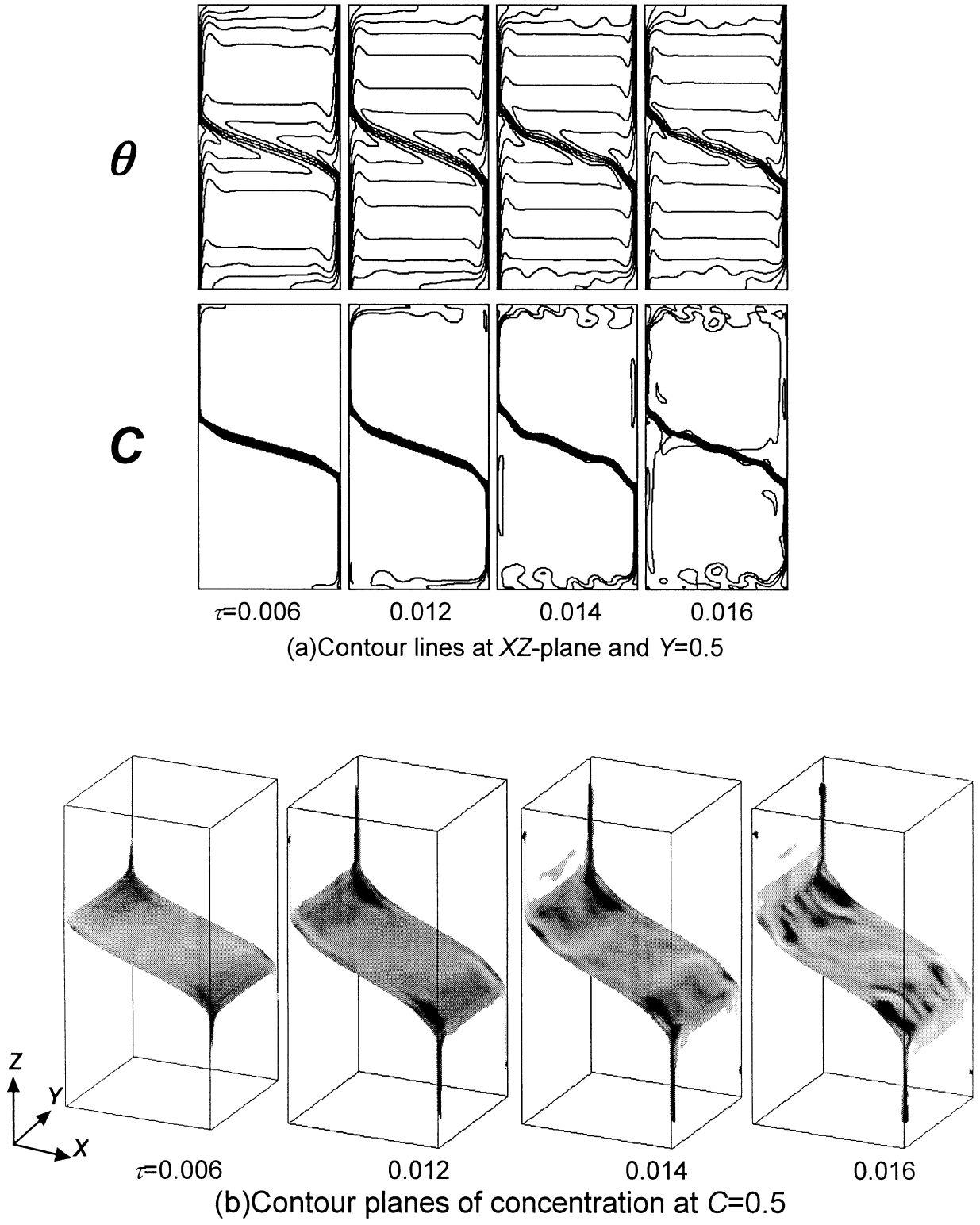

Fig. 8. Contour lines and planes at $N = 0.6$.

Ozoe [8]. At $Ra = 10^4$ the average Nusselt number Nu_{ave} on the hot or cold wall varied always monotonously with time. At $Ra = 10^5$ the Nu_{ave} exhibits double periodic oscillation. Then a long periodic oscillation corresponds to the periodical change of the concentration distribution in a layer and a short periodic oscillation corresponds to the flow oscillation which is caused by the periodic collapse of the balance of two kinds of buoyancies. At $Ra = 10^6 Nu_{ave}$ has single periodic oscillation corresponding to the flow oscillation.

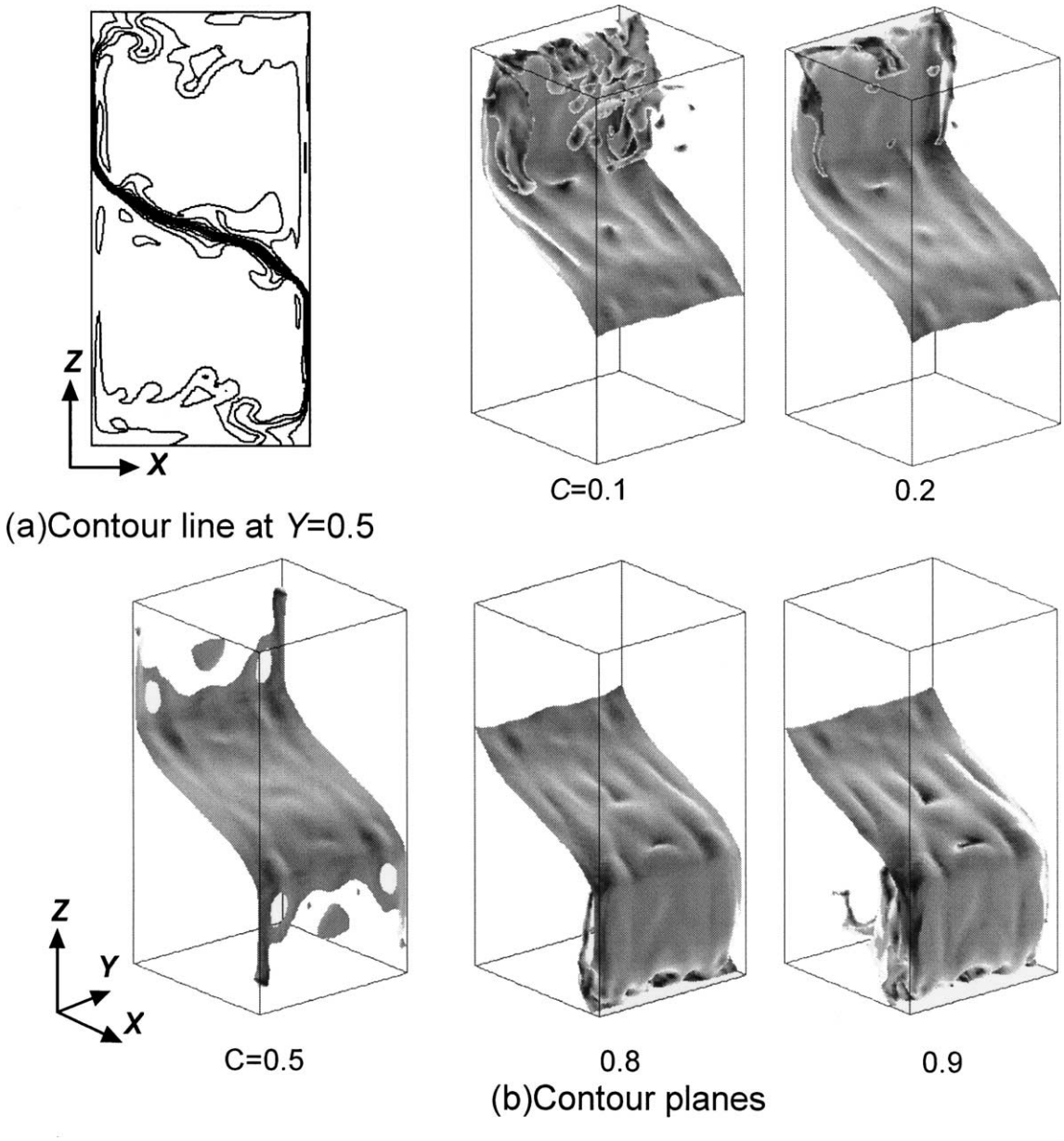

Fig. 9. Concentration distribution at $N = 0.6$ and $\tau = 0.02$.

The numerical calculations of double-diffusive natural convection in the two-layer system induced by lateral heating and cooling were carried out at $Pr = 6$, $Le = 100$, $A = 2$ and $Ra = 10^7$. Fig. 5 shows the average Nusselt number on the hot wall. The natural convection at $N = 0$ was monotonous but the oscillatory characteristic was found at $N > 0$. The Nu_{ave} at $N = 0.3$ was very low with oscillation at an early stage but became monotonous with time. However the value increased after $\tau \approx 0.01$ and will approach the Nu_{ave} values for $N = 0$. At $N = 0.6$ the Nu_{ave} became small gradually from $\tau \approx 0.003$ and then had distinct oscillation at $\tau > 0.011$. The Nu_{ave} at $N = 1$ showed almost regular oscillation after an induction time. This oscillation seems to correspond to the flow oscillation mentioned above. At $N = 3$ the amplitude became small after $\tau \approx 0.018$ and the oscillation of Nu_{ave} seems to be caused by the occurrence of the disordered flow in each layer as mentioned later.

3.2. Contour maps of concentration at $N = 0$

Fig. 6 shows a series of instantaneous contours of temperature and concentration at $N = 0$. The case of $N = 0$ means that the solutal buoyancy is zero, that is, very low concentration or very small density-difference between solution and water. For example, the small or no density difference occurs at aqueous solutions of organic salts. A flow is formed along the walls in the entire system and the stratified temperature distribution is formed from the bottom to the surface. As a result, the concentration attains a complicated distribution in the entire system with time.

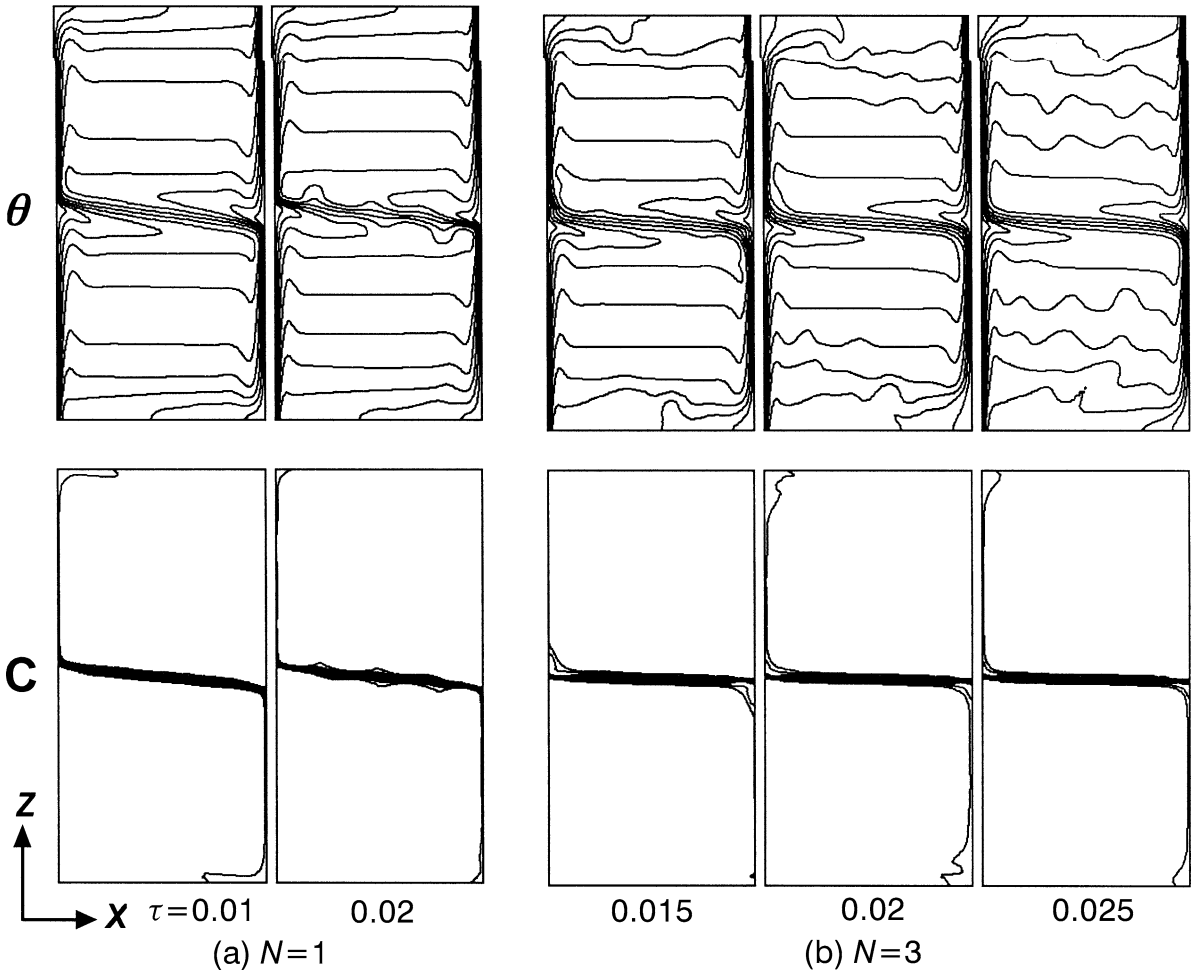

Fig. 10. Instantaneous contours at the XZ-plane, $N = 1$ and 3.

3.3. Contour maps of concentration at $N = 0.3$

Instantaneous contours of concentration at $N = 0.3$ are shown in Fig. 7(a). As thermal buoyancy is much larger than solutal buoyancy, each liquid in upper or lower layer penetrated into another layer along cold or hot wall, respectively. Consequently the liquid of high temperature and high concentration exists near the top and that of low temperature and low concentration exists near the bottom. These liquids near both the top and the bottom became unstable owing to the thermal conduction and salt-fingers with the termination of bulbous shapes were formed.

The salt-finger and the plumes are essentially three-dimensional phenomena which have the shape such as straight or crooked cylinder. Fig. 7(b) shows the concentration distribution at $N = 0.3$ and $\tau = 0.006$. The salt-fingers are seen in each layer.

3.4. Contour maps of concentration at $N = 0.6$

Fig. 8 shows the concentration distribution at $N = 0.6$. The flows which could penetrate into the other layer along the vertical walls are quite limited because the interface is more stable than that at $N = 0.3$. Therefore, the convection is limited mainly inside each layer, and the temperature is low just above the tilted interface and high just below the tilted interface. The contour plane was smooth at $\tau = 0.012$, but became uneven at $\tau = 0.014$. Later several plumes appeared above or below the interface as seen at $\tau = 0.016$ in Fig. 8(a). The plumes may occur owing to the collision of solutal fragments against the interface [5] as mentioned at the next section. Salt-fingers like the case of $N = 0.3$ were not observed because of the little amount of flow into the other layer. The plumes move with the main circulating flow along the tilted interface and approach the vertical walls. Finally the concentration distributions in the plumes were dispersed near the top surface or near the bottom, and the concentration in each layer becomes almost uniform.

The flow across the interface is observed near the corners as seen in Fig. 8(b) and the flows are able to make fingers, because four holes which seem to be made by the fingers exist near the corners. Fig. 9 shows the subsequent concentration distribution at $\tau = 0.02$. The contour plane at $C = 0.1$ indicates that the fragments of higher concentration are moving downwards owing to the gravity or with flow. A few solutal fragments which became small owing to the

dispersion may collide against the interface and then a plume occurs. When the interface is continuously bombarded, the shape of plumes becomes long in parallel to the flow as seen near the front or rear walls in the pictures.

3.5. Contour maps of concentration at $N = 1$

Instantaneous contours at $N = 1$ are shown in Fig. 10(a). The case of $N = 1$ means that the solutal buoyancy is equal to the thermal buoyancy. The inclination of the interface becomes small and two-layer system stable. However, very weak plumes exist as seen for a weak ragged interface. The plumes moved similarly to the case of $N = 0.6$ and the concentration distribution in the plumes was dispersed near the surface or near the bottom. The concentration inside each layer is almost uniform similarly to the case of $N = 0.6$.

3.6. Contour maps of concentration at $N = 3$

Instantaneous contours at $N = 3$ are shown in Fig. 10(b). The interface between two layers is a slightly tilted sharp one and convection occurs in each layer. The solute is transfered across the interface from the lower layer to the upper layer. The flux of solute is relatively small and the concentration distribution is uniform in each layer. The distorted temperature distribution in Fig. 10(b) seems to correspond to the weak oscillation of Nu_{ave} at $\tau > 0.018$ as shown at $N = 3$ in Fig. 5. When the concentration difference between two layers becomes small with the lapse of time, plumes or salt-fingers will occur as shown in Fig. 2.

4. Conclusions

Three-dimensional numerical calculations of double-diffusive natural convection were carried out for the two-layer system at $Pr = 6$, $Le = 100$, $A = 2$ and $Ra = 10^7$. Salt-fingers were formed owing to the penetration of convective flow in a layer into the other layer at $N = 0.3$ and plumes were formed by the collision of solutal fragments against the interface at $N = 0.6$ or 1. In the case of high buoyancy ratios, the interface was stable and salt-fingers and plumes did not exist in the solution system. However, the concentration difference between two layers becomes small with a lapse of time and then plumes and salt-fingers will occur similarly to the case of small buoyancy ratios.

References

[1] K. Kamakura, H. Ozoe, Double-diffusive natural convection between vertical parallel walls: Experimental study of two-layer convection, J. Chem. Engrg. Japan 24 (1991) 622–627.

[2] T.L. Bergman, A. Ungan, A note on lateral heating in a double-diffusive system, J. Fluid Mech. 194 (1988) 175–186.

[3] C.F. Chen, F. Chen, Salt-finger convection generated by lateral heating of a solute gradient, J. Fluid Mech. 352 (1997) 161–176.

[4] J. Tanny, B. Yakubov, Experimental study of a double-diffusive two-layer system in a laterally heated enclosure, Internat. J. Heat Mass Transfer 42 (1999) 3619–3629.

[5] M.T. Hyun, T.L. Bergman, Direct simulation of double-diffusive layered convection, ASME J. Heat Trans. 117 (1995) 334–339.

[6] T. Nishimura, Al.M. Morega, K. Kunitsugu, S. Sakura, Direct simulation of double-diffusive convection in a salt-stratified system, in: 5th ASME/JSME Joint Thermal Engrg. Conf., San Diego, AJTE99-6376, 1999.

[7] B.P. Leonard, A survey of finite differences with upwinding for numerical modeling of the incompressible convective diffusion equation, in: Computational Techniques in Transient and Turbulent Flow, Vol. 2, Pineridge Press, Swansea, 1981.

[8] K. Kamakura, H. Ozoe, Oscillatory double diffusive natural convection in a two-layer system, in: Proc. 10th Internat. Heat Transfer Conf., Vol. 7, 1994, pp. 67–72.